



Article

Toxic Metals in Particulate Matter and Health Risks in an E-Waste Dismantling Park and Its Surrounding Areas: Analysis of Three PM Size Groups

Yingjun Wu ^{1,2} , Guiying Li ^{1,2,*} and Taicheng An ^{1,2}

- ¹ Guangdong-Hong Kong-Macao Joint Laboratory for Contaminants Exposure and Health, Guangdong Key Laboratory of Environmental Catalysis and Health Risk Control, Institute of Environmental Health and Pollution Control, Guangdong University of Technology, Guangzhou 510006, China
- ² Guangzhou Key Laboratory of Environmental Catalysis and Pollution Control, Key Laboratory of City Cluster Environmental Safety and Green Development of the Ministry of Education, School of Environmental Science and Engineering, Guangdong University of Technology, Guangzhou 510006, China
- * Correspondence: ligy1999@gdut.edu.cn; Tel.: +86-153-233-43835

Abstract: Heavy metals generated from e-waste have created serious health risks for residents in e-waste disposal areas. This study assessed how airborne toxic metals from an e-waste dismantling park (EP) influenced surrounding residential areas after e-waste control. PM_{2.5}, PM₁₀, and total suspended particles (TSP) were sampled from 20 sites, including an EP, residential areas, and an urban site; ten kinds of metals were analyzed using ICP-MS and classified as PM_{2.5}, PM_{2.5–10}, and PM_{10–100}. Results showed that metals at the EP tended to be in coarser particles, while metals from residential areas tended to be in finer particles. A source analysis showed that metals from the EP and residential areas may have different sources. Workers' cancer and non-cancer risks were higher when exposed to PM_{2.5–10} metals, while residents' risks were higher when exposed to PM_{2.5} metals. As and Cr were the most strongly associated with cancer risks, while Mn was the most strongly associated with the non-cancer risk. Both workers and residents had cancer risks ($>1.0 \times 10^{-6}$), but risks were lower for residents. Therefore, e-waste control can positively affect public health in this area. This study provides a basis for further controlling heavy metal emissions into the atmosphere by e-waste dismantling and encouraging worldwide standardization of e-waste dismantling.

Keywords: heavy metals; size and spatial distribution; particulate matters; health risks; e-waste



Citation: Wu, Y.; Li, G.; An, T. Toxic Metals in Particulate Matter and Health Risks in an E-Waste Dismantling Park and Its Surrounding Areas: Analysis of Three PM Size Groups. *Int. J. Environ. Res. Public Health* **2022**, *19*, 15383. <https://doi.org/10.3390/ijerph192215383>

Academic Editor: Paul B. Tchounwou

Received: 28 September 2022

Accepted: 19 November 2022

Published: 21 November 2022

Publisher's Note: MDPI stays neutral with regard to jurisdictional claims in published maps and institutional affiliations.



Copyright: © 2022 by the authors. Licensee MDPI, Basel, Switzerland. This article is an open access article distributed under the terms and conditions of the Creative Commons Attribution (CC BY) license (<https://creativecommons.org/licenses/by/4.0/>).

1. Introduction

Many metals, including arsenic (As), cadmium (Cd), chromium (Cr), and nickel (Ni), are known carcinogens, and can lead to lung, skin, or bladder cancer [1]. These metals are also ubiquitous in multiple environments, including the atmosphere [2], water bodies [3], and soil [4]. Some non-carcinogenic metal ions, such as copper (Cu) and iron (Fe), can cause oxidative stress and can subsequently induce DNA damage, lipid peroxidation, protein modification, and other effects. These can lead to diseases including cancer, cardiovascular disease, and neurological disorders [5]. Metals can be absorbed through inhalation, dermal contact, and ingestion. Exposure through inhalation is somewhat inevitable, and can lead some metals, such as lead (Pb), to be deposited in the lungs for long periods [6]. These particles can then form insoluble and more toxic compounds, such as lead phosphate or iron–oxygen binding compounds [7]. In addition, as confirmed with one study using rats, inhaled metal-contained particles, such as uranium particles, can directly enter the brain [8]. This highlights the need to study metal exposure through the inhalation pathways. This includes studying both carcinogenic and non-carcinogenic metals in particulate matter (PM_{2.5}, PM₁₀, and total suspended particles (TSP)).

A growing body of research shows that toxic metal levels in biological samples, such as human blood and urine, are associated with metals from particulate matter [9,10].

Exposure to toxic metals causes different adverse health impacts for young people, such as respiratory symptoms and asthma [4,11,12], abnormal kidney function [13], and low birth weight in newborns [14]. Studies of older human populations have found that exposure to PM_{2.5}-bound toxic metals may cause premature death [15]. People living near industrial areas may face a higher risk of exposure to metals, due to atmospheric transmission [1,16]. High metal exposure levels have been reported in studies of several industries, including wire rope production [17], electroplating [18], and informal e-waste dismantling (home-style workshop, original dismantling such as acid leaching, and open fire burning) [19]. Several studies have reported that informal e-waste dismantling has generated serious metallic pollution in the surrounding environment, causing health problems, especially in developing countries [20,21]. Extremely high levels of heavy metals have been detected in atmospheric particulate matter, surface dust, and in soils from e-waste areas [22,23], leading to elevated Pb levels in blood [24].

Metal pollutants such as Pb, Cr, As, Cd, and Ni have been reported at high levels in e-waste dismantling areas in China [25,26]. Although China no longer imports e-waste, there remain large amounts of locally generated e-waste [27]. In southern China, a formal e-waste dismantling park (dismantling equipped with environmental protection devices with licenses) was built in 2016 to replace informal homestyle e-waste dismantling workshops in residential areas [28]. This government action was taken to prevent residents from being exposed to the pollutants emitted from e-waste dismantling. However, one study reported that high concentrations of Pb and Cr were detected near the formal e-waste recycling factory [29]. In addition, a recent study reported that children living near the formal e-waste dismantling area still suffered a carcinogenic health risk from metals in the soil [4].

Many organic pollutants have been found in the atmosphere and soil after the establishment of the government's formal e-waste dismantling park [30,31]; however, the metal pollution in environmental matrices other than soil has been somewhat limited [4]. Metals in soil generally accumulate over time, while those in the atmosphere are more recently produced. Thus, measuring toxic metals in the atmosphere is critical for evaluating contamination from recently produced metals, after the establishment of the formal e-waste dismantling park. Meanwhile, simultaneously investigating atmospheric metals in the surrounding residential areas of the e-waste dismantling park allows a further evaluation of the impact of formal e-waste on the surrounding area. It is particularly important to study metals of different particulate sizes, because finer particle sizes are associated with greater risks to human health [32].

Given this background, the purpose of this study was to investigate metal levels in particulate matter in residential areas surrounding the formal e-waste dismantling park in southern China. This was completed by collecting particulate matter from 18 sites distributed in communities or villages around the e-waste dismantling town on consecutive days. The typical metals associated with e-waste dismantling activities were analyzed using inductively coupled plasma mass spectrometry (ICP-MS). The metal size distribution was assessed by simultaneously collecting PM_{2.5}, PM₁₀, and TSP samples from one sampling site. In addition, a sampling site was set in the e-waste dismantling park to facilitate a correlation analysis of metals between the e-waste dismantling park and residential areas. Furthermore, a health risk assessment was conducted to evaluate the inhalation risks for residents and the e-waste dismantlers after the establishment of the formal e-waste dismantling park.

2. Materials and Methods

2.1. Study Site and Sample Collection

A total of 19 sampling sites, labeled as the EP site and sites S1–S18, were established at the e-waste area and in the town of Guiyu in Guangdong province, as shown in Figure S1. The weather on each sampling day during November 2017 is summarized in Table S1 and was reported in our previous study [31]. The subtropical monsoon climate in the study area is characterized by long summers and short winters and long rainy seasons. The EP

site was set in the e-waste dismantling park, near the dismantling workshops. In addition, one site was also set in a non-e-waste area (113°24'18" N, 23°02'35" E) to compare the pollutant levels between residential areas that were exposed and not exposed to e-waste. PM_{2.5}, PM₁₀, and TSP samples were simultaneously collected at each site, using three high-volume samplers at an airflow rate of 1.05 m³/min. The samplers were equipped with PM_{2.5}, PM₁₀, and TSP impactors, respectively (TH1000, Wuhan Tianhong Environmental Protection Industry Co., Ltd., Wuhan, China). Quartz fiber filters (203 mm × 254 mm, 1851-865, GE Whatman, Maidstone, UK) were used in the sampling loader; these were pretreated by baking them at 450 °C for 3 h to remove moisture and organic matter. Each sampling event was approximately 8 h in duration (from 9:00 to 17:00), with the sampler placed at approximately 1.5 m above the ground.

2.2. Sample Pretreatments and Instrumental Analysis

The mass concentrations of PM_{2.5}, PM₁₀, and TSP were determined by calculating the gravimetric differences between the filters before and after sampling at 25 °C and 20% humidity. One-eighth of each entirely membrane-loaded sample was cut into pieces using ceramic scissors. Each sample was then digested with a 10 mL acid solution, using fully enclosed microwave digestion (MARS6, CEM Corporation, Matthews, NC, USA) at 200 °C for 1 h. The digested acid consisted of 5.55% (v/v) HNO₃ (trace metal grade, A509-P212, Thermo Fisher Scientific Inc., Waltham, MA, USA) and 16.75% (v/v) HCl (for trace metal analysis (ppb), CFEQ-4-110005-00EA, CNW, ANPEL Laboratory Technologies Inc., Shanghai, China) in ultrapure water (specific resistance ≥ 18.25 M·cm). This metal analysis method was recommended by the Chinese Ministry of Environmental Protection (MEP) [33], and the temperature ramp-up procedure for microwave digestion was summarized in Table S2. The digested sample solution was diluted with 1% HNO₃ and was filtered through a 0.45 μm microporous membrane before the analysis. The ICP-MS (7900, Agilent Technology Co., Ltd., Santa Clara, CA, USA) was used to measure the concentrations of ten metals: Fe, Zn (zinc), Cu, Mn (manganese), Pb, V (vanadium), Ni, Cr, As, and Cd. A multi-element calibration standard solution was purchased from Agilent Technology Co., Ltd., Santa Clara, CA, USA (Lot#: 50-069CRY2). The working standard curve was developed using dilutions with 1% (v/v) HNO₃; the correlations exceeded 0.999. In addition, Sc (scandium), In (indium), and Bi (bismuth) (Lot#: 50-024CRY2, Agilent Technology Co., Ltd., Santa Clara, CA, USA) were used as the internal standard, using a peristaltic pump for matrix correction.

The concentration of each metal in the particulate matter (C_{air} , ng/m³) was calculated according to Equation (1).

$$C_{\text{air}} = (C - C_0) \times V_s \times \frac{n}{v} \quad (1)$$

where C and C_0 (ng/L) represent the sample and blank metal concentrations' digestion acid solution, respectively. V_s (L) represents the constant volume of the digestion solution; and v represents the sampling air volume at an ambient temperature (m³). The n is the digested proportion of the total sample filter area.

2.3. Source Apportionment Analysis

A principal component analysis (PCA) and cluster analysis are suitable multi-variate approaches for environmental-based research studies [34]. The PCA is a commonly used model to identify the sources of heavy metals in soil and particulate matter [35–37]. The PCA is a dimensionality reduction algorithm that obtains the main factors and provides the weights (loading scores) of heavy metals for each component [38]. The study adopted the first two factors to be retained, and then a varimax rotation was performed.

A cluster analysis is another dimensionality reduction algorithm that obtains the information among metals in the same categories [39]. In this study, systematic cluster analysis was conducted for metals grouping from the same source. In addition, the correlation coefficient measures the strength of the inter-relationship, which in this study, was the

possibility of the same source, between two heavy metals [34]. A Spearman correlation analysis was conducted for the non-linear correlation analysis [31].

2.4. Human Health Risk Assessment via Inhalation

The United States Environmental Protection Agency's (US EPA) current methodology for health assessment is described in a previous study [40]. The health risks associated with metals in PM_{2.5} and PM_{2.5-10} (with a dynamic diameter between 2.5 and 10 µm, obtained by subtracting the PM_{2.5} concentration from the PM₁₀ concentration) samples were assessed for their ability to be inhaled; metals in PM₁₀₋₁₀₀ (with a dynamic diameter between 10 and 100 µm, obtained by subtracting the PM₁₀ concentration from the TSP concentration) samples were considered non-inhalable. In this study, the adjusted air concentration (C_{air-adj}) was used as the exposure concentration (EC) of populations. The C_{air-adj} of each metal was calculated using Equation (2), obtained from the EPA website accessed on 30 June 2022 (<https://www.epa.gov/expobox/exposure-assessment-tools-routes-inhalation>). The EC of Cr was adjusted to 0.034 times of the total Cr [41], because the reference concentration (RfC) and inhalation unit risk (IUR) could be obtained only for hexavalent Cr. The metals Cu, Zn, and Fe were excluded from the health risk assessment, because they had no associated RfC and IUR. Previous studies found that workers in the e-waste dismantling park generally worked 10 h a day, 6 days a week [42]. To facilitate comparisons under the same conditions, the same exposure timing and frequency were used for both workers and residents.

The lifetime cancer risk (LCR) values and hazard quotients (HQ) were the representative terms used for the quantitative evaluation. The LCR is the probability of cancer when exposed to the toxicant. An HQ value or hazard index (HI, or the sum of multiple toxicant HQs) of less than 1 indicates there is no threat to a sensitive population [43]. The RfC and IUR values from the United States Integrated Risk Information System (US IRIS) are used to calculate LCR and HI (Equations (3)–(5)).

$$EC = C_{\text{air-adj}} = C_{\text{air}} \times 10^{-3} \times ET \times \frac{1 \text{ day}}{24 \text{ hour}} \times EF \times \frac{ED}{AT} \quad (2)$$

$$LCR = IUR \times EC \quad (3)$$

$$HQ_i = \frac{EC}{RfC_i} \quad (4)$$

$$HI = \sum HQ_i \quad (5)$$

where EC is the exposure concentration (µg/m³); and C_{air} is the concentration of metal in the atmospheric environment (ng/m³). ET represents the exposure time (hours/day), set at 10 h; EF represents the exposure frequency (days/year), set at 288 days/year; ED represents exposure duration (in years), set at 24 years; and AT represents the average time (day) of exposure, calculated by ED × 365 days for non-carcinogens and 70 years × 365 days/year for carcinogens [44]. The chemical forms of metals in the air used to select IUR_i (mg/m³) and RfC_i ((µg/m³)⁻¹) are shown in Table S3.

2.5. Statistical Analysis

IBM SPSS Statistics 13.0 software (SPSS Inc., Chicago, IL, USA) was used for the statistical analysis. The geometric mean with standard deviation was used to represent particulate matter and its metal concentrations in residential areas. This approach was used because the data were not normally distributed, based on the Shapiro–Wilk test (Table S4). A Spearman correlation analysis and PCA were used to investigate the sources of metals in particulate matter. The spatial maps were drawn using ArcGIS 10.2. (GeoScene Information Technology Co., Ltd., Beijing, China). The cluster analysis and data display diagrams were created using Origin Pro 2022 (learning version, OriginLab Corporation, Northampton, NC, USA).

2.6. Quality Assurance and Quality Control

All sample containers were soaked with 20% (*v/v*) HNO₃ overnight, rinsed with ultra-pure water (>18.25 Ω), and then dried to protect them from environmental pollution. An internal standard was used to correct for matrix interference and drift. Metal concentrations in samples were corrected using the average of three procedure blanks for every batch, which were treated in the same way as the samples. The recovery of spiked metals (50 µg/L) in the blank quartz filters was 81.57–92.91%, and the detailed information was provided in Table S5. Results were corrected using the average concentration of the background levels in the 7 quartz fiber filters.

3. Results and Discussion

3.1. PM_{2.5}, PM₁₀, and TSP Pollution in E-Waste Area

Table 1 shows the mass concentrations of PM_{2.5}, PM₁₀, and TSP. The findings of the descriptive analysis show that the PM_{2.5} concentration (mean) was highest at the EP site (131.75 µg/m³), followed by the urban site (89.30 µg/m³) and residential areas (median: 70.01 µg/m³ and geomean: 77.08 ± 30.31 µg/m³). However, some residential areas observed very high PM_{2.5} (147.92 µg/m³) exposure with a wide range (39.12–147.92 µg/m³).

Table 1. Mass concentrations of PM_{2.5}, PM₁₀, and TSP, and relevant metal concentrations.

Element	EP Site Mean	Surrounding Residential Area		Urban Site Mean
		Geomean (±SD *)	Median (Range)	
PM _{2.5} (µg/m ³)	131.75	77.08 (±30.31)	70.01 (39.12–147.92)	89.30
As (ng/m ³)	4.48	3.51 (±1.99)	3.85 (1.46–8.80)	3.25
Cd (ng/m ³)	1.75	1.19 (±0.5)	1.47 (0.49–2.08)	0.56
Pb (ng/m ³)	162.90	27.93 (±12.02)	31.28 (10.09–53.24)	18.52
Cr (ng/m ³)	8.36	6.36 (±4.68)	6.84 (2.11–23.28)	9.35
Mn (ng/m ³)	54.54	21.53 (±12.96)	21.90 (9.74–59.33)	33.75
V (ng/m ³)	5.33	2.82 (±1.33)	2.77 (1.04–5.35)	18.71
Ni (ng/m ³)	18.59	3.01 (±2.3)	2.69 (1.29–9.73)	9.66
Zn (ng/m ³)	308.25	95.61 (±60)	101.96 (15.14–242.26)	156.75
Cu (ng/m ³)	122.11	36.76 (±62.64)	35.85 (3.09–195.76)	71.56
Fe (ng/m ³)	1607.38	1016.07 (±1.99)	552.92 (244.72–1425.39)	375.89
PM ₁₀ (µg/m ³)	235.28	116.67 (±40.68)	103.08 (83.27–182.30)	111.93
As (ng/m ³)	7.21	5.24 (±2.85)	4.93 (1.85–10.92)	4.60
Cd (ng/m ³)	3.74	1.72 (±0.76)	1.76 (0.56–3.45)	0.82
Pb (ng/m ³)	419.38	44.32 (±16.16)	41.95 (19.03–90.86)	48.51
Cr (ng/m ³)	23.00	10.41 (±3.78)	9.73 (6.85–21.01)	13.17
Mn (ng/m ³)	131.33	48.89 (±15.62)	47.30 (29.87–85.38)	51.57
V (ng/m ³)	9.95	5.6 (±1.93)	5.60 (3.06–11.50)	23.36
Ni (ng/m ³)	47.87	5.27 (±2.12)	4.90 (3.54–10.26)	15.27
Zn (ng/m ³)	758.01	170. (±41)	163.18 (43.51–357.35)	214.39
Cu (ng/m ³)	287.99	66.81 (±101.45)	68.61 (8.17–368.75)	59.43
Fe (ng/m ³)	4771.38	1763.88 (±2.85)	1503.17 (986.84–4010.48)	1136.26
TSP (µg/m ³)	457.42	183.78 (±104.83)	155.42 (106.71–411.34)	128.47
As (ng/m ³)	12.67	6.39 (±2.64)	7.33 (2.88–11.43)	5.07
Cd (ng/m ³)	6.19	2.04 (±0.67)	2.24 (0.88–3.37)	0.84
Pb (ng/m ³)	1224.95	54.28 (±17.59)	56.18 (24.55–92.29)	67.78
Cr (ng/m ³)	36.77	17.81 (±5.63)	18.42 (11.51–36.01)	19.73
Mn (ng/m ³)	295.21	86.06 (±44.43)	77.89 (45.88–196.36)	61.25
V (ng/m ³)	15.60	7.66 (±4.46)	6.72 (4.33–23.26)	21.74
Ni (ng/m ³)	126.30	8.72 (±3.7)	9.04 (4.46–18.09)	18.10
Zn (ng/m ³)	1636.70	250.29 (±104.12)	248.36 (113.33–505.69)	266.25
Cu (ng/m ³)	1126.66	70.11 (±77.67)	75.95 (11.45–315.66)	75.75
Fe (ng/m ³)	15,309.03	1507.04 (±2.64)	2623.64 (1470.36–11,297.02)	1727.61

* SD: standard deviation.

The results of PM_{10} and TSP were a bit different from $PM_{2.5}$. The highest PM_{10} and TSP concentrations were recorded at the EP site (PM_{10} : $235.28 \mu\text{g}/\text{m}^3$, TSP: $457.42 \mu\text{g}/\text{m}^3$), followed by residential areas (geomean: PM_{10} : $116.67 \mu\text{g}/\text{m}^3$, TSP: $183.78 \mu\text{g}/\text{m}^3$), and the urban site (PM_{10} : $111.93 \mu\text{g}/\text{m}^3$, TSP: $128.47 \mu\text{g}/\text{m}^3$). However, like $PM_{2.5}$, the highest PM_{10} concentration was observed in residential areas ($182.30 \mu\text{g}/\text{m}^3$). Furthermore, the $PM_{2.5}$, PM_{10} , and TSP concentrations in all areas exceeded China's air quality standard (AQS) guidelines (GB 3095-2012) [45], and European Commission AQS ($25 \mu\text{g}/\text{m}^3$ for $PM_{2.5}$) (https://environment.ec.europa.eu/topics/air/air-quality/eu-air-quality-standards_en, accessed on 30 June 2022) guidelines.

Figure 1 shows the size fraction of particulate matter in the samples from each sampling site in the e-waste area. The three sites with the highest PM_{10-100} concentrations were EP, S11, and S18. The weather may have played a role because it was cloudy on the sampling day (Table S1). However, there was no relationship between the concentrations at the EP site and the weather; it was a sunny day during sampling. All of these results indicate that PM_{10-100} made up the largest size fraction of PM in this e-waste area, while $PM_{2.5}$, $PM_{2.5-10}$, and PM_{10-100} pollution were all significant. This highlighted the need to further investigate the composition of the particulate matter.

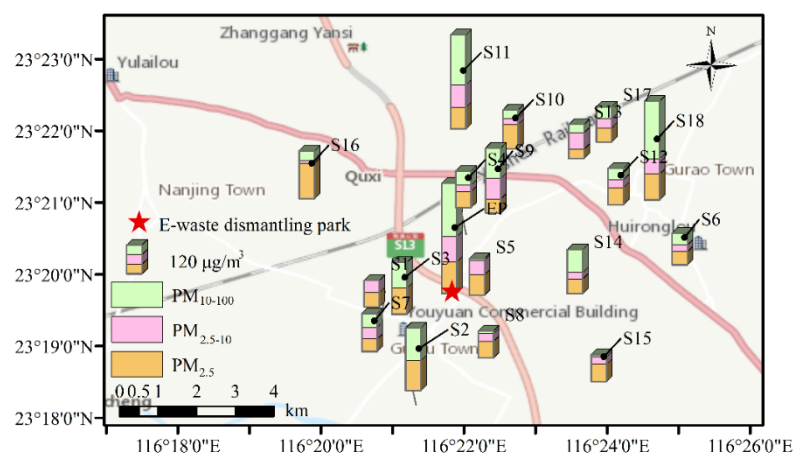


Figure 1. The spatial map of $PM_{2.5}$, $PM_{2.5-10}$, and PM_{10-100} concentrations in the e-waste dismantling park and the surrounding residential area. S1–S18 and EP were labels of sampling points.

3.2. Metal Pollution Profile in $PM_{2.5}$, PM_{10} , and TSP

Ten typical metals found in the e-waste area were further analyzed in the $PM_{2.5}$, PM_{10} , and TSP samples (Table 1). The highest concentration of metals was observed at the EP site. All samples showed the highest concentration of Fe and the lowest concentration of Cd. Among the three PM sizes, the highest concentration for all metals was observed in the TSP. Figure S2 shows each metal concentration at each sampling site in the residential areas. Though the mean concentrations of analyzed metals were higher in EP samples than in residential areas, some metals showed very high concentrations in the residential area. Atmospheric V in the e-waste area of this study (maximum $23.26 \text{ ng}/\text{m}^3$) indicated light pollution, at similar levels as cities in China ($17.9 \pm 16.5 \text{ ng}/\text{m}^3$) [46]. With the exception of V, no other analyzed metal in the TSP was highest in the residential area.

The individual metal concentrations were compared with the national and international guidelines or standards. The metal limit values or guidelines from the current AQS of China (contains Pb, As, and Cd), European Commission (contains Pb, As, Cd, and Mn), and WHO [47] (contains Pb, As, Cd, Ni, and V) are as follows: Pb: $0.5 \mu\text{g}/\text{m}^3$, Cd: $5 \text{ ng}/\text{m}^3$, As: $6 \text{ ng}/\text{m}^3$, Mn: $150 \text{ ng}/\text{m}^3$, Ni: $20 \text{ ng}/\text{m}^3$, and V: $1000 \text{ ng}/\text{m}^3$. For samples from the residential area, only As in some sample sites exceeded the above limit, showing As pollution at some residential sites. For the EP site, all the metals in the TSP sample exceeded the guidelines, e.g., As, Cd, Pb, Mn, and Ni were present at levels that were 2.11, 1.24, 2.49, 1.97, and 6.31 times higher than the AQS or WHO limits, respectively. In the PM_{10}

sample, Ni ($47.87 \mu\text{g}/\text{m}^3$) and As ($7.21 \text{ ng}/\text{m}^3$) exceeded the limit. Unfortunately, there is no standardization or guidelines for Cr, Zn, Cu, and Fe in atmospheric PM, indicating that the actual metal pollution may be more severe within the EP and residential areas.

Compared to the metal concentrations in samples from an informal e-waste dismantling informal workshop collected for a previous study, before the centralized dismantling of e-waste [22], Cd, Pb, and Zn concentrations in TSP samples at the EP site decreased sharply, from 80 to $4.54 \text{ ng}/\text{m}^3$ (Cd), 4.42 to $1.03 \mu\text{g}/\text{m}^3$ (Pb), and 3.32 to $1.37 \mu\text{g}/\text{m}^3$ (Zn). Fe concentrations in TSP samples decreased slightly, from 11.49 to $10.81 \mu\text{g}/\text{m}^3$. In contrast, Ni, Mn, and Cu concentrations increased from 80 to $111.12 \text{ ng}/\text{m}^3$ (Ni), 160 to $257.03 \text{ ng}/\text{m}^3$ (Mn), and 540 to $749.79 \mu\text{g}/\text{m}^3$ (Cu), and do not have limits under China's AQS. These results indicate that the formalization of centralized e-waste dismantling may help reduce Cd, Pb, and Zn concentrations in TSP from the EP site.

In addition, the $\text{PM}_{2.5}$ bound metal concentrations in residential areas of this study were compared with those of the informal e-waste dismantling period in 2004 and 2012–2013 [48,49], when the informal e-waste workshops were mainly scattered in residential areas [50]. Cu, Zn, Pb, Cr, Ni, and Cd levels in $\text{PM}_{2.5}$ decreased to 0.6% (Cr)–84% (Cd) of those in 2004, in which samples were collected on the third floor of the building near the e-waste baking site [48]. However, Mn concentrations remained at similar levels in the residential areas of this study compared to those in 2004. In addition, Pb and Cd also decreased to 17% (Pb) and 21% (Cd) of those in 2012–2013, but Cr and Mn increased to 1.12 (Cr) and 1.27 (Mn) times [49]. Thus, Mn may not be the characteristic metal of e-waste dismantling activities.

Ni and Pb may be the characteristic metals of e-waste dismantling activities. Ni compounds are classified as Class 1 carcinogens by the International Agency for Research on Cancer, meaning that the chemical is a known human carcinogen [51]. In the informal e-waste dismantling period of 2007, Ni in TSP samples ranged from 50 to $150 \text{ ng}/\text{m}^3$ [22], indicating that formalization of e-waste dismantling may not reduce Ni emissions. However, Ni from the EP site did not spread to the residential areas, where the Ni concentration was found to be below the limit in this study. The particularly high concentration of Ni at the EP site may be caused by the specific e-waste type. In another e-waste dismantling area, Qingyuan, China, the sum of Ni concentrations in size-fraction particles was 3.5 to $19 \text{ ng}/\text{m}^3$ [25], which was significantly lower than levels detected in samples from the EP site in this study. Ni comes from the stainless steel and printed circuit boards of e-waste [52]. The mechanical cutting of bulky printed boards may lead to high Ni levels in TSP samples from the EP site, while Ni concentrations in $\text{PM}_{2.5}$ samples were lower than the limit.

Pb presented at the second highest levels, above the AQS limit. Heavy air Pb pollution has been found in e-waste areas across China (maximum of $1000 \text{ ng}/\text{m}^3$ in $\text{PM}_{2.5}$ samples) [49] and India (maximum of $2000 \text{ ng}/\text{m}^3$ Pb in $\text{PM}_{2.5}$ samples) [53]. Herein, Pb concentrations at the EP site were significantly lower than those from the informal e-waste area (2.5 to $5.8 \mu\text{g}/\text{m}^3$) [22], but still exceeded the limit ($500 \text{ ng}/\text{m}^3$). Pb is mainly generated from the soldering of the components adhering to the printed circuit boards [23]. With the elimination of lead-acid batteries and use of lead-free soldering in China, Pb may decrease in e-waste in the future. However, lead-acid batteries are still used and dismantled in India, which may be a driver for high Pb pollution in the air in India. As with Ni, Pb in residential areas did not exceed the limit; however, reduced Pb concentrations in TSP indicate that the development of formal e-waste dismantling may reduce Pb emissions [22].

In sum, Cd, Pb, Ni, Zn, Cu, and Fe in $\text{PM}_{2.5}$ decreased after e-waste control, but Mn and Cr seemed to remain at similar levels. Formally dismantling and recycling e-waste support reductions in most toxic metals in $\text{PM}_{2.5}$ on the e-waste dismantling site and residential area.

3.3. Size Fraction of the Toxic Metals in $\text{PM}_{2.5}$, $\text{PM}_{2.5-10}$, and PM_{10-100}

In this study, the simultaneously sampled $\text{PM}_{2.5}$, PM_{10} , and TSP were further analyzed to determine the size fraction of metals in $\text{PM}_{2.5-10}$ and PM_{10-100} categories. This can

help evaluate different health effects, because different particle sizes can be deposited in different depths of the lung [54]. Figure 2 shows the size fractions of the metals in the samples from the EP site, the surrounding residential area (geomean), and the urban site. Figures S2 and S3 show the size fractions for the metals from each site in the residential area. The metal concentrations in TSP samples were set at a baseline 100%; as such, the proportion of each metal in PM_{2.5}, PM_{2.5–10}, and PM_{10–100} samples was expressed as a percentage of the concentration in TSP.

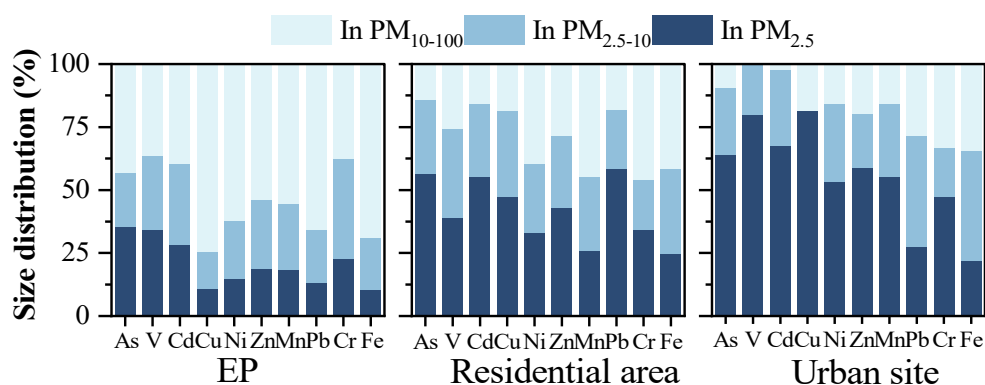


Figure 2. Size distribution of metals in e-waste dismantling park (EP), residential area (geomean of S1–S18), and one urban site.

In samples from the EP site, nine metals (not including Cr) were present at the highest proportions (36.21–74.44%) in the PM_{10–100} samples. Cr was distributed at a similar proportion in PM_{2.5–10} and PM_{10–100} samples (39.81% and 37.45%). Metals distributed in the PM_{2.5–10} samples made up about 14.72–39.81%; and As, V, and Cd were present at a higher proportion in the PM_{2.5} samples (28.30–35.33%) compared to other metals (10.84–22.74%). Compared with the previous study of the informal dismantling e-waste site, the proportions of Cd, Cr, Ni, Pb, Zn, Mn, and As in PM_{2.5} (43.9–108.3%) [48] were much higher than those in this study. This may be because e-waste was previously roasted over an open flame in an informal e-waste dismantling process, so the fine particles may have been generated by those combustion activities [55]. Generally, As, V, Cd, Cu, Ni, Zn, Mn, Pb, and Fe in samples from the EP site were more highly distributed in PM_{10–100}, which is considered to be a non-inhalable fraction. However, the coarse particles or dust may cause ingestion risks, due to pulmonary ciliary clearance after inhalation [56].

In samples from the residential area, the proportions of metals in the coarser particles were reduced. Metals in the PM_{10–100} proportion (14.17–45.94%) were lower in the surrounding residential area compared to at the EP site. Otherwise, metals in PM_{2.5} were higher in the surrounding residential area compared to the EP site. As, Cd, and Pb had the highest proportions in the PM_{2.5} samples (56.52%, 55.09%, and 58.32%, respectively), while the other metals had higher proportions in the PM_{2.5} samples (24.65–51.10%) from the residential sites compared to the samples from the EP site. Meanwhile, the metal proportions in PM_{2.5–10} were similar to those in residential areas (19.85–33.80%) and the EP site. Further, metals were distributed at the highest levels in PM_{2.5} samples from the urban site, at between 21.76% and 80.08%. This showed that urban domestic sources emitted mainly finer-sized metal particles. This is consistent with previous research results from the Pearl Delta area of China [40]. Thus, the elevated proportion of metal in finer particles from residential areas indicates the higher domestic sources' contribution. However, there are also geographic reasons for different ratios of metal distributions in fine particles. For example, higher humidity levels in coastal areas may cause the faster dry settlement of PM_{10–100} [57,58].

Finer particles cause more harm to exposed populations [59]. As such, even if metal concentrations are lower than the guidelines or limits in residential areas, the combined toxicity from multiple pollutants may not be low, due to the limited number of metals

analyzed for this study. Metals from e-waste dismantling activities tend to be distributed in coarser particles (PM_{10-100}), while metals in residential areas tend to be distributed in finer particles ($PM_{2.5}$ and $PM_{2.5-10}$). The different size distribution of metals may show diverse emission sources in the EP site and residential area.

3.4. Source Analysis

The Spearman correlation coefficients among metals are summarized in Table S6 (EP site) and Table S7 (surrounding residential area). The metals' levels were significantly correlated ($p < 0.05$), indicating that certain paired metals may have the same source [31]. In samples from the EP site, the Spearman correlations of all pairwise comparisons of Cd, Pb, Mn, Ni, Zn, Cu, and Fe were significantly correlated; the Spearman correlation of As and V was also significant. Cr was not significantly correlated with the other metals. Figure 3A shows that the PCA revealed results that were consistent with the Spearman correlation results: Cd, Pb, Mn, Ni, Zn, Cu, and Fe were sorted into one class; As and V were sorted into another class; and Cr was sorted into its own class. This indicates that Cd, Pb, Mn, Ni, Zn, Cu, Fe, and Cr were mainly affected by principal component (PC) 1. As and V were mainly affected by PC 2, but they were also affected by PC 1. The PCA scores of metals with respect to size fraction (in $PM_{2.5}$, $PM_{2.5-10}$, and PM_{10-100}) were low (<1) in each PC, which were close to each other (Figure 3A, triangle labels). This indicates that the metals detected in $PM_{2.5}$, $PM_{2.5-10}$, and PM_{10-100} samples from the EP site were likely from the same source, considered as e-waste dismantling activities.

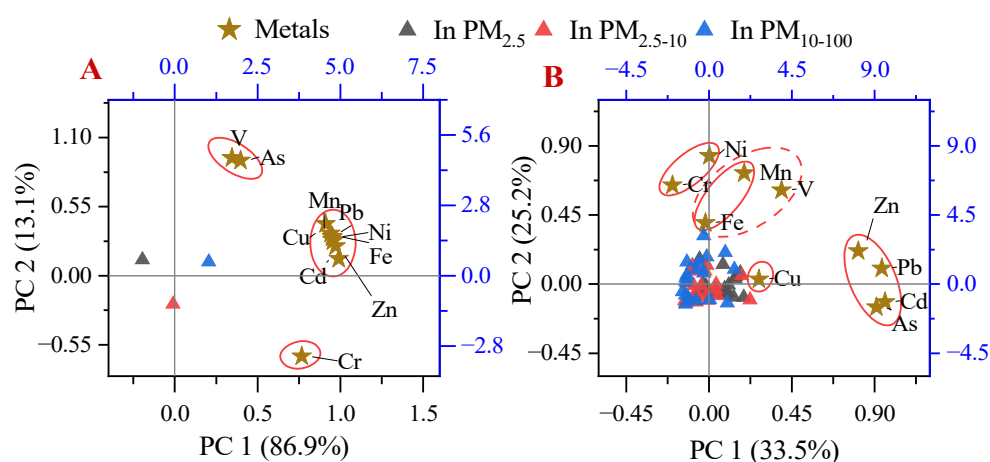


Figure 3. Principal component analysis of the metals in the e-waste dismantling park (A) and the surrounding residential area (B); principal components and related rotational load are in black, and the scores of the classification are in blue.

In previous studies, higher Cd, Pb, Mn, Ni, Zn, Cu, Fe, and Cr concentrations were found in the e-waste area [22,48]. However, Wu et. al. reported that As was likely not generated from e-waste dismantling activities, because there was no difference in the As concentration across the distances between dust sampling sites [60]. As and V have been reported as coexisting in drinking water, and can be caused by the corrosion of pipes or from by-products created from disinfecting drinking water [61]. Thus, the higher concentrations of coexisting As and V may have come from corroded metal waste. Cr is the main material in stainless steel [62], which is also present at high levels in e-waste.

Based on the discussion above, e-waste dismantling was likely the source of PC 1, given that all analyzed metals were related to e-waste material. Metal pipe corrosion may be the source of PC 2; this corrosion did occur in the e-waste dismantling park. However, the three classifications of metals had loadings in PC 1, with a cumulative variance of 86.9%. It indicates that metals detected at the EP site were mainly from e-waste dismantling activities, with the main metal pollutants being Cd, Pb, Mn, Ni, Zn, Cu, and Fe.

Determining the source of metals in residential areas is quite complicated. The Spearman correlation analysis (Table S7) found that As, Cd, Pb, and Zn were significantly correlated with each other in pairwise matching ($r > 0.50$, $p < 0.01$), and Ni was significantly correlated with Cr ($r = 0.86$). Some other metals were also significantly correlated with each other, but with an $r < 0.50$. The PCA (Figure 3B) and cluster analysis (Figure S4) were further applied to determine possible sources. PC 1 and PC 2 differed for samples in the surrounding residential area compared to those in the EP site. Metals were not divided into different groups by size fractions; this indicates they were affected by the same sources. The cumulative variances of PCs 1 and 2 were 33.5% and 25.2%, respectively, indicating that PC 1 and PC 2 were the main sources. However, other sources were also important contributors of metals in the residential area. For example, Zn, Pb, Cd, and As were grouped as a class with high loadings on PC 1, but were also clustered as their own class. Thus, Zn, Pb, Cd, and As were likely co-emitted from the same source in the surrounding residential area. Cu was isolated as its own class, indicating that it was not co-emitted with other metals in the residential area. The PCA result (classification of metals) was further confirmed by the cluster analysis, and the Spearman correlation of metals in the same class was significant ($p < 0.05$).

Figure S5 shows the spatial distribution of each metal in the study area. The figure also shows that the weak diffusion pattern of the metals extended from the EP site to the surrounding residential area in the downwind direction (northeast). The areas with higher As, Cd, and Zn concentrations (northwest and southeast) covered two roads. Most metals in the city were caused by traffic emissions [63]; and biomass combustion was also an important source of metals, especially Zn, Pb, Cd, and As [64]. However, the Pb levels did not show the same significant trends as seen for Zn, Cd, and As, due to the relatively high Pb concentration at the EP site. As discussed previously, metals from the EP site tended to be in coarser particles, which can weakly diffuse. Though extremely high Pb was from the EP site, limited Pb could diffuse to the surrounding area. Thus, PC 1 identified in the residential area may come from a traffic source. Moreover, Ni and Cr were generally co-emitted, as they are associated with a common group of stainless-steel materials, which differ from the e-waste dismantling source. Mn and Fe were also generally co-emitted, due to the common combination of iron and steel, and from vehicle wear or metal peeling. V was also grouped with Mn and Fe, which are also present in heavy oils [65,66]. All these indicate that these metals in residential areas may be more related to traffic emissions than e-waste.

3.5. Inhalation Health Risk Assessment

For adults, Figure 4A,B show the LCR and HQ associated with toxic metals in PM_{2.5} and PM_{2.5-10} samples. Here, the same exposure time and exposure frequency (e-waste dismantling workers' working periods) were used to assess adult health risk. The LCR of each carcinogenic metal differed between the PM_{2.5} and PM_{2.5-10} samples. At the EP site, the LCRs associated with Cd, Pb, Cr, and Ni were higher for the PM_{2.5-10} samples compared to the PM_{2.5} samples. In contrast, the LCR associated with As was higher in the PM_{2.5} samples compared to the PM_{2.5-10} samples. However, in the surrounding residential areas, the LCRs associated with all five carcinogenic metals were higher in PM_{2.5} samples compared to in PM_{2.5-10} samples. The same trends seen for As, Cd, Cr, and Ni were also seen for the metal HQ. A higher Mn HQ was seen in the PM_{2.5-10} samples, and a similar V HQ was seen in samples from both the EP site and residential sites (Figure 4B). The accumulated LCR and HI in samples from both the EP and residential areas (Figure 4C,D) further indicated that cancer and non-cancer risks for workers may be from the metals in PM_{2.5-10}, while risks for residents may be caused by the metals in PM_{2.5}.

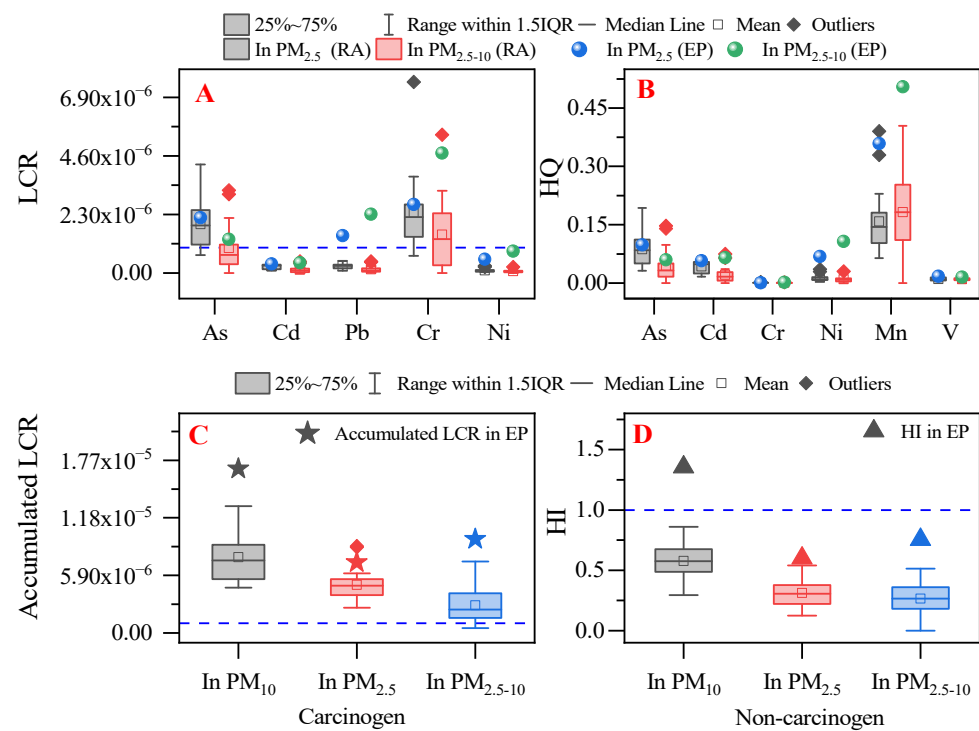


Figure 4. Life cancer risks (LCR) of single metal (A), hazards quotient (HQ) of single metal (B), the accumulated LCR of five metals (C), and hazards index (HI or accumulated HQ) of six metals (D) in PM_{2.5} and PM_{2.5-10}. EP: e-waste dismantling park; RA: the surrounding residential areas; the blue dash lines: the safe threshold of LCR and HI.

Among the five carcinogenic metals found at the EP site, the LCR was highest for Cr, followed in descending order by Pb > As > Ni > Cd. The LCR in residential areas was also highest for Cr, followed in descending order by As > Cd ≈ Pb ≈ Ni. Each single carcinogenic metal exceeded the safe threshold of cancer risk (the blue dash in Figure 4A,C, marking the level of 1.0×10^{-6} [56]). Exceptions included Cd and Ni at the EP site and residential area sites, and Pb at the residential area sites. However, the accumulated LCR values for the EP site and residential area sites exceeded the safe threshold (Figure 4C). These results indicated that the people working in the EP and living in the surrounding residential areas were exposed to unsafe levels of cancer risk. As and Cr were the most reported carcinogenic metals in the e-waste area. These metals were also reported as the leading causes of cancer risk from soil exposure for children in this area [4].

Figure 4B shows that the HQ of each metal was less than 1, indicating that workers and residents do not appear to have a heightened non-cancer risk from a single metal. Of the six metals, the HQ of Mn was associated with the highest non-cancer risk; it was mainly present in the PM_{2.5-10} samples. The HI did not exceed 1, except for the worker's HI in the PM₁₀ samples (the sum of HI values associated with the metal in the PM_{2.5} and PM_{2.5-10} samples). This indicates that Mn may be associated with the highest non-cancer risk at the EP site. However, many metals were excluded from the health risk assessment given the absence of an RfC or IUR. Furthermore, the analysis did not consider other exposure scenarios, such as indoor exposure. Therefore, the public health risks in this e-waste area still need research attention, especially with respect to cancer risks.

The study has some strengths and limitations. The study provides the first evidence that the formal e-waste control replacing the scattered homestyle e-waste dismantling workshop helped to prevent the residents from exposure to e-waste metal pollution. The study employs three different sizes of segregated PM sampling and the analysis of ten different metals including important metal pollutants. The study includes sampling from different residential sites to overcome the uncertainty of metal exposure in a residential

area. Nevertheless, the study also has some limitations. The study did not use the source apportionment models for source identification, which could have led to source misclassification. In addition, the lack of real-time meteorological information, such as wind speed and terrain conditions, also increased the challenge of source identification.

4. Conclusions

This study investigated the influence of airborne metals emitted from an e-waste site on surrounding residential areas, in the first year after the introduction of formal e-waste control. Metals emitted from e-waste dismantling activities tended to be distributed in coarser particles, and Pb, Ni, Fe, Mn, Zn, Cu, and Cd were detected in the e-waste site. A size and spatial analysis found that metals from the EP site had a slight impact on the surrounding residential areas. A source analysis further indicated that formal e-waste control actions have helped prevent the further spread of metals from the EP site to surrounding residential areas, likely reducing public health risks. However, exposure to metals in indoor environments may lead to more serious health risks for people, especially in e-waste dismantling workshops. Future studies should analyze indoor airborne metals to generate a more realistic exposure risk level, to identify the source of risk, and to inform mechanisms for reducing associated public health risks.

Supplementary Materials: The following supporting information can be downloaded at: <https://www.mdpi.com/article/10.3390/ijerph192215383/s1>. Figure S1. Research site and sampling spots in e-waste area; Figure S2. Metal concentration in each site of the e-waste surrounding residential area; Figure S3. Size distribution of metals in each site in the residential areas of e-waste area; Figure S4. The cluster analysis of metals in the surrounding residential area; the same color represents the primary cluster; Figure S5. Spatial distribution of metal in TSP, PM10 and PM2.5 in e-waste dismantling park (the location of cross) and surrounding residential areas; wind direction is mainly northeast; Table S1. The longitude and latitude of sampling spots; Table S2. Digestion program of microwave-assisted acid digestion method Video; Table S3. The selected metals IUR and RfC values for health risk assessment; Table S4. The Shapiro-Wilk normality test of metals concentration in size fraction in the surrounding residential area in e-waste area; Table S5. The recovery of metals in the blank quartz fiber filters with spiked 50 µg/L metals; Table S6. The Spearman correlation of metals in e-waste dismantling park; Table S7. The Spearman correlation coefficients of metals in the residential area surrounding the e-waste dismantling park.

Author Contributions: Data investigation and analysis, Y.W.; methodology, Y.W. and G.L.; Project administration, T.A.; writing—original draft preparation, Y.W.; writing—review and editing, Y.W., G.L. and T.A. All authors have read and agreed to the published version of the manuscript.

Funding: This work was financially supported by the National Key Research and Development Project (2019YFC1804504 and 2019YFC1804503), National Natural Science Foundation of China (41731279), and Local Innovative and Research Teams Project of Guangdong Pearl River Talents Program (2017BT01Z032).

Institutional Review Board Statement: Not applicable.

Informed Consent Statement: Not applicable.

Data Availability Statement: Not applicable.

Conflicts of Interest: The authors declare that there are no competing financial interests.

References

1. Straif, K.; Benbrahim-Tallaa, L.; Baan, R.; Grosse, Y.; Secretan, B.; El Ghissassi, F.; Bouvard, V.; Guha, N.; Freeman, C.; Galichet, L.; et al. A review of human carcinogens—Part C: Metals, arsenic, dusts, and fibres. *Lancet. Oncol.* **2009**, *10*, 453–454. [[CrossRef](#)]
2. Liu, M.; Wang, W.; Li, J.; Wang, T.; Xu, Z.; Song, Y.; Zhang, W.; Zhou, L.; Lian, C.; Yang, J.; et al. High fraction of soluble trace metals in fine particles under heavy haze in central China. *Sci. Total Environ.* **2022**, *841*, 156771. [[CrossRef](#)]

3. Feng, X.; Shao, L.; Jones, T.; Li, Y.; Cao, Y.; Zhang, M.; Ge, S.; Yang, C.X.; Lu, J.; BeruBe, K. Oxidative potential and water-soluble heavy metals of size-segregated airborne particles in haze and non-haze episodes: Impact of the “Comprehensive Action Plan” in China. *Sci. Total Environ.* **2022**, *814*, 152774. [[CrossRef](#)] [[PubMed](#)]
4. Yang, Y.; Zhang, M.; Chen, H.; Qi, Z.; Liu, C.; Chen, Q.; Long, T. Estimation of Children’s Soil and Dust Ingestion Rates and Health Risk at E-Waste Dismantling Area. *Int. J. Environ. Res. Public Health* **2022**, *19*, 7332. [[CrossRef](#)]
5. Jomova, K.; Valko, M. Advances in metal-induced oxidative stress and human disease. *Toxicology* **2011**, *283*, 65–87. [[CrossRef](#)] [[PubMed](#)]
6. Kastury, F.; Smith, E.; Doelsch, E.; Lombi, E.; Donnelley, M.; Cmielewski, P.L.; Parsons, D.W.; Scheckel, K.G.; Paterson, D.; de Jonge, M.D.; et al. In Vitro, in Vivo, and Spectroscopic Assessment of Lead Exposure Reduction via Ingestion and Inhalation Pathways Using Phosphate and Iron Amendments. *Environ. Sci. Technol.* **2019**, *53*, 10329–10341. [[CrossRef](#)]
7. Kastury, F.; Smith, E.; Lombi, E.; Donnelley, M.W.; Cmielewski, P.L.; Parsons, D.W.; Noerpel, M.; Scheckel, K.G.; Kingston, A.M.; Myers, G.R.; et al. Dynamics of Lead Bioavailability and Speciation in Indoor Dust and X-ray Spectroscopic Investigation of the Link between Ingestion and Inhalation Pathways. *Environ. Sci. Technol.* **2019**, *53*, 11486–11495. [[CrossRef](#)]
8. Ibanez, C.; Suhard, D.; Elie, C.; Ebrahimian, T.; Lestaavel, P.; Roynette, A.; Dhieux-Lestaavel, B.; Gensdarmes, F.; Tack, K.; Tessier, C. Evaluation of the Nose-to-Brain Transport of Different Physicochemical Forms of Uranium after Exposure via Inhalation of a UO₄ Aerosol in the Rat. *Environ. Health Perspect.* **2019**, *127*, 97010. [[CrossRef](#)]
9. Eriksen Hammer, S.; Dorn, S.L.; Dartey, E.; Berlinger, B.; Thomassen, Y.; Ellingsen, D.G. Occupational Exposure among Electronic Repair Workers in Ghana. *Int. J. Environ. Res. Public Health* **2022**, *19*, 8477. [[CrossRef](#)]
10. Wu, Y.; Yang, X.; Wang, H.; Jia, G.; Wang, T. Relationship between ambient PM_{2.5} exposure and blood cadmium level in children under 14 years in Beijing, China. *J. Hazard. Mater.* **2021**, *403*, 123871. [[CrossRef](#)]
11. Zeng, X.; Xu, X.; Boezen, H.M.; Huo, X. Children with health impairments by heavy metals in an e-waste recycling area. *Chemosphere* **2016**, *148*, 408–415. [[CrossRef](#)] [[PubMed](#)]
12. Farzan, S.F.; Howe, C.G.; Chen, Y.; Gilbert-Diamond, D.; Cottingham, K.L.; Jackson, B.P.; Weinstein, A.R.; Karagas, M.R. Prenatal lead exposure and elevated blood pressure in children. *Environ. Int.* **2018**, *121*, 1289–1296. [[CrossRef](#)] [[PubMed](#)]
13. Yang, F.; Yi, X.; Guo, J.; Xu, S.; Xiao, Y.; Huang, X.; Duan, Y.; Luo, D.; Xiao, S.; Huang, Z.; et al. Association of plasma and urine metals levels with kidney function: A population-based cross-sectional study in China. *Chemosphere* **2019**, *226*, 321–328. [[CrossRef](#)] [[PubMed](#)]
14. Jiang, M.; Li, Y.; Zhang, B.; Zhou, A.; Zheng, T.; Qian, Z.; Du, X.; Zhou, Y.; Pan, X.; Hu, J. A nested case-control study of prenatal vanadium exposure and low birthweight. *Human Reprod.* **2016**, *31*, 2135. [[CrossRef](#)]
15. Liu, J.; Cao, H.; Zhang, Y.; Chen, H. Potential years of life lost due to PM_{2.5}-bound toxic metal exposure: Spatial patterns across 60 cities in China. *Sci. Total Environ.* **2022**, *812*, 152593. [[CrossRef](#)]
16. Li, W.; Wang, T.; Zhou, S.; Lee, S.; Huang, Y.; Gao, Y.; Wang, W. Microscopic observation of metal-containing particles from Chinese continental outflow observed from a non-industrial site. *Environ. Sci. Technol.* **2013**, *47*, 9124–9131. [[CrossRef](#)]
17. Chen, K.; Huang, L.; Yan, B.; Li, H.; Sun, H.; Bi, J. Effect of lead pollution control on environmental and childhood blood lead level in Nantong, China: An interventional study. *Environ. Sci. Technol.* **2014**, *48*, 12930–12936. [[CrossRef](#)]
18. Wu, L.L.; Gong, W.; Shen, S.P.; Wang, Z.H.; Yao, J.X.; Wang, J.; Yu, J.; Gao, R.; Wu, G. Multiple metal exposures and their correlation with monoamine neurotransmitter metabolism in Chinese electroplating workers. *Chemosphere* **2017**, *182*, 745–752. [[CrossRef](#)]
19. Zheng, L.; Wu, K.; Li, Y.; Qi, Z.; Han, D.; Zhang, B.; Gu, C.; Chen, G.; Liu, J.; Chen, S.; et al. Blood lead and cadmium levels and relevant factors among children from an e-waste recycling town in China. *Environ. Res.* **2008**, *108*, 15–20. [[CrossRef](#)]
20. Zeng, X.; Gong, R.; Chen, W.Q.; Li, J. Uncovering the Recycling Potential of “New” WEEE in China. *Environ. Sci. Technol.* **2016**, *50*, 1347–1358. [[CrossRef](#)]
21. Awasthi, A.K.; Zeng, X.; Li, J. Environmental pollution of electronic waste recycling in India: A critical review. *Environ. Pollut.* **2016**, *211*, 259–270. [[CrossRef](#)] [[PubMed](#)]
22. Bi, X.H.; Simoneit, B.R.T.; Wang, Z.Z.; Wang, X.M.; Sheng, G.Y.; Fu, J.M. The major components of particles emitted during recycling of waste printed circuit boards in a typical e-waste workshop of South China. *Atmos. Environ.* **2010**, *44*, 4440–4445. [[CrossRef](#)]
23. Leung, A.O.; Duzgoren-Aydin, N.S.; Cheung, K.C.; Wong, M.H. Heavy metals concentrations of surface dust from e-waste recycling and its human health implications in southeast China. *Environ. Sci. Technol.* **2008**, *42*, 2674–2680. [[CrossRef](#)] [[PubMed](#)]
24. Bo, Z.; Xia, H.; Long, X.; Cheng, Z.; Cong, X.; Lu, X.; Xu, X. Elevated lead levels from e-waste exposure are linked to decreased olfactory memory in children. *Environ. Pollut.* **2017**, *231*, 1112–1121.
25. Huang, C.L.; Bao, L.J.; Luo, P.; Wang, Z.Y.; Li, S.M.; Zeng, E.Y. Potential health risk for residents around a typical e-waste recycling zone via inhalation of size-fractionated particle-bound heavy metals. *J. Hazard. Mater.* **2016**, *317*, 449–456. [[CrossRef](#)]
26. Zeng, X.; Xu, X.; Zheng, X.; Reponen, T.; Chen, A.; Huo, X. Heavy metals in PM_{2.5} and in blood, and children’s respiratory symptoms and asthma from an e-waste recycling area. *Environ. Pollut.* **2016**, *210*, 346–353. [[CrossRef](#)] [[PubMed](#)]
27. Rautela, R.; Arya, S.; Vishwakarma, S.; Lee, J.; Kim, K.H.; Kumar, S. E-waste management and its effects on the environment and human health. *Sci. Total Environ.* **2021**, *773*, 145623. [[CrossRef](#)] [[PubMed](#)]
28. Tang, Y. Pollution: Centralized pilot for e-waste processing. *Nature* **2016**, *538*, 41. [[CrossRef](#)]

29. Fang, W.; Yang, Y.; Xu, Z. PM10 and PM2.5 and health risk assessment for heavy metals in a typical factory for cathode ray tube television recycling. *Environ. Sci. Technol.* **2013**, *47*, 12469–12476. [CrossRef]
30. Ge, X.; Ma, S.; Zhang, X.; Yang, Y.; Li, G.; Yu, Y. Halogenated and organophosphorous flame retardants in surface soils from an e-waste dismantling park and its surrounding area: Distributions, sources, and human health risks. *Environ. Int.* **2020**, *139*, 105741. [CrossRef]
31. Yue, C.; Ma, S.; Liu, R.; Yang, Y.; Li, G.; Yu, Y.; An, T. Pollution profiles and human health risk assessment of atmospheric organophosphorus esters in an e-waste dismantling park and its surrounding area. *Sci. Total Environ.* **2022**, *806*, 151206. [CrossRef] [PubMed]
32. Wang, W.; Lin, Y.; Yang, H.; Ling, W.; Liu, L.; Zhang, W.; Lu, D.; Liu, Q.; Jiang, G. Internal Exposure and Distribution of Airborne Fine Particles in the Human Body: Methodology, Current Understandings, and Research Needs. *Environ. Sci. Technol.* **2022**, *56*, 6857–6869. [CrossRef] [PubMed]
33. HJ-657-2013; Ambient Air and Stationary Source Emission—Determination of Metals in Ambient Particulate Matter—Inductively Coupled Plasma/Mass Spectrometry (ICP-MS). Ministry of Ecology and Environment of the People’s Republic of China: Beijing, China, 2013.
34. Lu, X.; Wang, L.; Li, L.Y.; Lei, K.; Huang, L.; Kang, D. Multivariate statistical analysis of heavy metals in street dust of Baoji, NW China. *J. Hazard. Mater.* **2010**, *173*, 744–749. [CrossRef] [PubMed]
35. Anaman, R.; Peng, C.; Jiang, Z.C.; Liu, X.; Zhou, Z.R.; Guo, Z.H.; Xiao, X.Y. Identifying sources and transport routes of heavy metals in soil with different land uses around a smelting site by GIS based PCA and PMF. *Sci. Total Environ.* **2022**, *823*, 153759. [CrossRef] [PubMed]
36. Taner, S.; Pekey, B.; Pekey, H. Fine particulate matter in the indoor air of barbeque restaurants: Elemental compositions, sources and health risks. *Sci. Total Environ.* **2013**, *454–455*, 79–87. [CrossRef]
37. Zhai, Y.; Liu, X.; Chen, H.; Xu, B.; Zhu, L.; Li, C.; Zeng, G. Source identification and potential ecological risk assessment of heavy metals in PM2.5 from Changsha. *Sci. Total Environ.* **2014**, *493*, 109–115. [CrossRef]
38. Zhang, Y.; Li, S.; Chen, Z.; Wang, F.; Chen, J.; Wang, L. A systemic ecological risk assessment based on spatial distribution and source apportionment in the abandoned lead acid battery plant zone, China. *J. Hazard. Mater.* **2018**, *354*, 170–179. [CrossRef]
39. Kumar, P.; Fulekar, M.H. Multivariate and statistical approaches for the evaluation of heavy metals pollution at e-waste dumping sites. *SN Appl. Sci.* **2019**, *1*, 1506. [CrossRef]
40. Wu, Y.; Li, G.; Yang, Y.; An, T. Pollution evaluation and health risk assessment of airborne toxic metals in both indoors and outdoors of the Pearl River Delta, China. *Environ. Res.* **2019**, *179*, 108793. [CrossRef]
41. Yu, C.H.; Huang, L.; Shin, J.Y.; Artigas, F.; Fan, Z.H. Characterization of concentration, particle size distribution, and contributing factors to ambient hexavalent chromium in an area with multiple emission sources. *Atmos. Environ.* **2014**, *94*, 701–708. [CrossRef]
42. An, T.; Huang, Y.; Li, G.; He, Z.; Chen, J.; Zhang, C. Pollution profiles and health risk assessment of VOCs emitted during e-waste dismantling processes associated with different dismantling methods. *Environ. Int.* **2014**, *73*, 186–194. [CrossRef] [PubMed]
43. EPA. *Risk Assessment Guidance for Superfund*; U.S. Environmental Protection Agency: Washington, DC, USA, 1989; Volume I.
44. Hu, X.; Zhang, Y.; Ding, Z.; Wang, T.; Lian, H.; Sun, Y.; Wu, J. Bioaccessibility and health risk of arsenic and heavy metals (Cd, Co, Cr, Cu, Ni, Pb, Zn and Mn) in TSP and PM2.5 in Nanjing, China. *Atmos. Environ.* **2012**, *57*, 146–152. [CrossRef]
45. GB 3095-2012; Ambient Air Quality Standards. MEP: Beijing, China, 2012.
46. Duan, J.; Tan, J. Atmospheric heavy metals and Arsenic in China: Situation, sources and control policies. *Atmos. Environ.* **2013**, *74*, 93–101. [CrossRef]
47. WHO, Regional Office for Europe. *Air Quality Guidelines for Europe*, 2nd ed.; World Health Organization, Regional Office for Europe: København, Denmark, 2000; Available online: <https://apps.who.int/iris/handle/10665/107335> (accessed on 30 June 2022).
48. Deng, W.J.; Louie, P.K.K.; Liu, W.K.; Bi, X.H.; Fu, J.M.; Wong, M.H. Atmospheric levels and cytotoxicity of PAHs and heavy metals in TSP and PM2.5 at an electronic waste recycling site in southeast China. *Atmos. Environ.* **2006**, *40*, 6945–6955. [CrossRef]
49. Zheng, X.B.; Xu, X.J.; Yekeen, T.A.; Zhang, Y.L.; Chen, A.M.; Kim, S.S.; Dietrich, K.N.; Ho, S.M.; Lee, S.A.; Reponen, T.; et al. Ambient Air Heavy Metals in PM2.5 and Potential Human Health Risk Assessment in an Informal Electronic-Waste Recycling Site of China. *Aerosol Air. Qual. Res.* **2016**, *16*, 388–397. [CrossRef]
50. Wong, M.H.; Wu, S.C.; Deng, W.J.; Yu, X.Z.; Luo, Q.; Leung, A.O.; Wong, C.S.; Luksemburg, W.J.; Wong, A.S. Export of toxic chemicals—A review of the case of uncontrolled electronic-waste recycling. *Environ. Pollut.* **2007**, *149*, 131–140. [CrossRef]
51. IARC. *Arsenic, Metals, Fibres, and Dusts. A Review of Human Carcinogens*; WHO Press: Lyon, France, 2012; Volume 100C.
52. Priya, A.; Hait, S. Toxicity characterization of metals from various waste printed circuit boards. *Process Saf. Environ.* **2018**, *116*, 74–81. [CrossRef]
53. Shen, H.; Peters, T.M.; Casuccio, G.S.; Lersch, T.L.; West, R.R.; Kumar, A.; Kumar, N.; Ault, A.P. Elevated Concentrations of Lead in Particulate Matter on the Neighborhood-Scale in Delhi, India As Determined by Single Particle Analysis. *Environ. Sci. Technol.* **2016**, *50*, 4961–4970. [CrossRef]
54. Heyder, J.; Gebhart, J.; Rudolf, G.; Schiller, C.F.; Stahlhofen, W. Deposition of particles in the human respiratory tract in the size range 0.005–15 μm . *J. Aerosol Sci.* **1986**, *17*, 811–825. [CrossRef]

55. Zhou, J.Z.; Wu, S.M.; Pan, Y.; Zhang, L.G.; Cao, Z.B.; Zhang, X.Q.; Yonemochi, S.; Hosono, S.; Wang, Y.; Oh, K.; et al. Enrichment of heavy metals in fine particles of municipal solid waste incinerator (MSWI) fly ash and associated health risk. *Waste Manag.* **2015**, *43*, 239–246. [[CrossRef](#)]
56. Gao, P.; Guo, H.; Zhang, Z.; Ou, C.; Hang, J.; Fan, Q.; He, C.; Wu, B.; Feng, Y.; Xing, B. Bioaccessibility and exposure assessment of trace metals from urban airborne particulate matter (PM10 and PM2.5) in simulated digestive fluid. *Environ. Pollut.* **2018**, *242*, 1669–1677. [[CrossRef](#)]
57. Seinfeld, J.H.; Pandis, S.N. *Atmospheric Chemistry and Physics: From Air Pollution to Climate Change*, 3rd ed.; John Wiley & Sons: Hoboken, NJ, USA, 2016.
58. Wu, S.P.; Li, X.; Cai, M.J.; Gao, Y.; Xu, C.; Schwab, J.J.; Yuan, C.S. Size distributions and health risks of particle-bound toxic elements in the southeast coastland of China. *Environ. Sci. Pollut. Res. Int.* **2021**, *28*, 44565–44579. [[CrossRef](#)]
59. Hetland, R.B.; Myhre, O.; Lag, M.; Hongve, D.; Schwarze, P.E.; Refsnes, M. Importance of soluble metals and reactive oxygen species for cytokine release induced by mineral particles. *Toxicology* **2001**, *165*, 133–144. [[CrossRef](#)]
60. Wu, Y.; Li, Y.; Kang, D.; Wang, J.; Zhang, Y.; Du, D.; Pan, B.; Lin, Z.; Huang, C.; Dong, Q. Tetrabromobisphenol A and heavy metal exposure via dust ingestion in an e-waste recycling region in Southeast China. *Sci. Total Environ.* **2016**, *541*, 356–364. [[CrossRef](#)]
61. Flint, L.C.; Arias-Paic, M.S.; Korak, J.A. Removal of hexavalent chromium by anion exchange: Non-target anion behavior and practical implications. *Environ. Sci.-Water Res. Technol.* **2021**, *7*, 2397–2413. [[CrossRef](#)]
62. Thomann, O.; Pihlatie, M.; Schuler, J.A.; Himanen, O.; Kiviaho, J. Method for Measuring Chromium Evaporation from SOFC Balance-of-Plant Components. *Electrochem. Solid State Lett.* **2012**, *15*, B35–B37. [[CrossRef](#)]
63. Hou, S.N.; Zheng, N.; Tang, L.; Ji, X.F.; Li, Y.Y.; Hua, X.Y. Pollution characteristics, sources, and health risk assessment of human exposure to Cu, Zn, Cd and Pb pollution in urban street dust across China between 2009 and 2018. *Environ. Int.* **2019**, *128*, 430–437. [[CrossRef](#)]
64. Cheng, K.; Wang, Y.; Tian, H.; Gao, X.; Zhang, Y.; Wu, X.; Zhu, C.; Gao, J. Atmospheric emission characteristics and control policies of five precedent-controlled toxic heavy metals from anthropogenic sources in China. *Environ. Sci. Technol.* **2015**, *49*, 1206–1214. [[CrossRef](#)]
65. Agrawal, H.; Eden, R.; Zhang, X.; Fine, P.M.; Katzenstein, A.; Miller, J.W.; Ospital, J.; Teffera, S.; Cocker, D.R., III. Primary particulate matter from ocean-going engines in the Southern California Air Basin. *Environ. Sci. Technol.* **2009**, *43*, 5398–5402. [[CrossRef](#)] [[PubMed](#)]
66. Tao, J.; Zhang, L.; Cao, J.; Zhong, L.; Chen, D.; Yang, Y.; Chen, D.; Chen, L.; Zhang, Z.; Wu, Y.; et al. Source apportionment of PM2.5 at urban and suburban areas of the Pearl River Delta region, south China—With emphasis on ship emissions. *Sci. Total Environ.* **2017**, *574*, 1559–1570. [[CrossRef](#)]